Structural Characterization of the pH-Denatured States of Ferricytochrome-c by Synchrotron Small Angle X-Ray Scattering

Stefania Cinelli,* Francesco Spinozzi,† Rosangela Itri,‡ Stephanie Finet,§ Flavio Carsughi,¶ Giuseppe Onori,* and Paolo Mariani†

*Dipartimento di Fisica and INFM, Università di Perugia, Via Pascoli, I-06123 Perugia, Italy; †Istituto di Scienze Fisiche and INFM, Università di Ancona, Via Ranieri 65, I-60131 Ancona, Italy; ‡Instituto de Fisica, Universitade de Sao Paulo, CP 66318, Sao Paulo SP05315-970, Brasil; §ESRF-sector 03–03.1.04, BP 220, 38043 Grenoble cedex, France; and ¶Dipartimento di Scienze e Biotecnologie Agrarie ed Ambientali, and INFM, Università di Ancona, Via Brecce Bianche, I-60131, Ancona, Italy

ABSTRACT The ferricytochrome-c (cyt-c) shows a complex unfolding pathway characterized by a series of stable partially folded states. When titrated with HCl at low ionic strength, two transitions are detected. At pH 2, cyt-c assumes the U_1 unfolded state, whereas the successive addition of Cl^- ion from either HCl or NaCl induces the recompaction to a molten globule conformation (A_1 and A_2 states, respectively). A second unfolded state (U_2) is also observed at pH 12. Recent data evidence different features for the local structure of the heme in the different states. To derive relationships between local and overall conformations, we analyzed the structural characteristics of the different states by synchrotron small angle x-ray scattering. The results show that in the acidic-unfolded U_1 form the protein assumes a worm-like conformation, whereas in the alkaline-unfolded U_2 state, the cyt-c is globular. Moreover, the molten globule states induced by adding HCl or NaCl to U_1 appear structurally different: in the A_1 state cyt-c is dimeric and less compact, whereas in the A_2 form the protein reverts to a globular-like conformation. According to the local heme structure, a molecular model for the different forms is derived.

INTRODUCTION

The present work deals with a study of the structural properties of partially folded states of ferricytochrome-c (cyt-c) in acidic and alkaline solutions using small angle x-ray scattering (SAXS) by synchrotron radiation sources.

Determination of the structural characteristics of partially folded intermediate state in proteins is crucial for understanding the mechanism of folding and the principle of structure stabilization. Among partially denatured states, the molten globule has been devoted of a special interest. The molten globule is a compact denatured protein form, with a significantly native-like secondary structure but a largely flexible and disordered tertiary structure. On the basis of structural and kinetic studies, the molten globule has been proposed as the major intermediate in globular protein folding (Goto et al., 1990a,b; Christensen and Pain, 1991).

Horse cyt-c is a well characterized globular protein both in the crystalline and in solution states and it represents a very useful model for protein folding studies (Scott and Mauk, 1996). In particular, cyt-c has been shown to exist in three stable states in acidic pH region, corresponding to the native (N), unfolded (U_1) and compact intermediate or molten globule (A) forms (Goto et al., 1990a; Ohgushi and Wada, 1983; Fink et al., 1994), and in one unfolded state stable at alkaline pH (the U_2 state). In recent years, the U_2 form has been the object of extensive studies, especially in connection with the role of conformational changes in electron transfer (Wilson and Greenwood, 1996; Döpner et al., 1998; Rossel at al., 1998; Weber at al., 1987).

The structural properties of the cyt-c unfolded states have been mainly analyzed in terms of gyration radii and of changes in protein compactness also using time-resolution techniques (Kataoka et al., 1993; Banci et al., 1999; Pollack et al., 1999). Moreover, the definition of the conformational characteristics of the molten globule form is still an open problem. In fact, acid-unfolding of cyt-c occurs substantially under conditions of low salt at pH 2 (U_1 state); the subsequent addition of Cl^- ion from either HCl or NaCl induces the recompaction to a molten globule state, indicating that the chloride anion should play a key role in acid-salt induced refolding. The state induced by addition of more acid is defined as A_1 state, whereas the compact intermediate state obtained by addition of NaCl at pH 2 is the A_2 state (Boffi et al., 2001). The unfolding/refolding pathways of cyt-c is then sketched below:

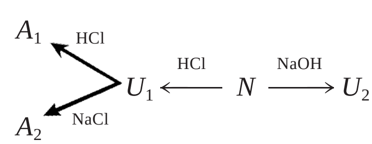

Optical and circular dichroism spectroscopy showed that the two intermediate states A_1 and A_2 have similar secondary structure (Goto et al., 1990a,b). In a recent work, x-ray absorption spectroscopy (XAS) at Fe K-edge has been used to characterize the local environment of the heme iron of cyt-c in acidic and basic conditions (Boffi et al., 2001): the comparison of XAS protein spectra with experimental model systems showed that local site structures of the two intermediate states induced by adding HCl (A_1) or NaCl (A_2)

Received for publication 14 May 2001 and in final form 19 September 2001.

Address reprint requests to Dr. Francesco Spinozzi, Istituto di Scienze Fisiche, Facoltà di Medicina, Università di Ancona, Via Ranieri 65, I-60131 Ancona, Italy. Tel.: 39-071-2204608; Fax: 39-071-2204605; E-mail: f.spinozzi@alisf1.unian.it.

0006-3495/01/12/3522/12 $2.00

to the HCl denatured state (U_1) are different. These results indicate that the formation of a native-like secondary structure induced both by acid and salt is not related to the coordination at the heme pocket level. This prompt us to reexamine this question by using a more direct probe than the optical spectroscopy to characterize the partially folded states of cyt-c.

SAXS is ideally suitable to this purpose (Trewhella, 1997; Pérez et al., 2001 and reference therein). Note that while XAS is a short-range probe sensitive to variations in the local structure, SAXS is a powerful tool for analyzing the size and the shape of protein molecules, thus information on the relationship between local and overall conformation can be obtained by the coordinated use of both techniques. In this work, SAXS has been then used to characterize the size and the shape of cyt-c in all the stable states *N*, *U*, and *A*. Moreover optical absorption measurements have been performed to monitor the pH and salt induced transitions between them.

MATERIALS AND METHODS

Cytochrome-c

Cyt-c is a well-know monomeric protein with a molecular mass of 12,000 Da, as calculated from the amino acids composition. The protein dry volume and averaged electron density, also derived from the amino acid composition using data reported by Jacrot and Zaccai (Jacrot, 1976; Jacrot and Zaccai, 1981), are 14,500 $\AA^3$ and 0.438 e $\AA^{-3}$, respectively. The theoretical radius of gyration, $R_{g,th}$, calculated as indicated below from the atomic coordinates, is 12.6 Å.

Horse heart cyt-c (type III) has been obtained from Sigma (St. Louis, MO). Samples for both SAXS and optical absorption measurements have been prepared dissolving the dry powder in bidistilled water. To remove all the ions eventually contained in the commercial powder, the solution has been subsequently dialyzed overnight against bidistilled water. After dialysis, the samples have been diluted to the appropriate concentration of 0.8 mM (corresponding to $c = 10$ g l^{-1}). Final samples have been prepared from the same native water solution by adding negligible volumes of high concentrated acid-basic-salt solutions to reach the required molar ratios; consequently, the added volumes did not change appreciably the protein concentration. pH measurements and titrations have been made using a Crison micro-pH 2000 pH-meter.

The experimental procedure has been the following: 1) a pH titration has been carried out on the protein from pH 7 to 12 using NaOH; 2) a pH titration has been carried out on the protein from pH 7 to 0.5 using HCl in absence of salt; 3) a salt titration with NaCl has been carried out over 0 to 500 mM range at the pH of maximal unfolding (40 mM HCl at pH $\sim$ 2).

Optical absorption measurements

All absorption spectroscopy measurements have been performed using the JASCO V-750 instrument. The concentration of native cyt-c has been determined on suitable dilute protein samples using extinction coefficient ϵ of 1.06 10^5 M^{-1} cm^{-1} at 410 nm and 25°C. To make a comparison with folding studies based on structural probes, the conformational transitions of cyt-c have been studied at 695 nm ($\epsilon = 810$ M^{-1} cm^{-1}) and at 620 nm ($\epsilon =$ 1100 M^{-1} cm^{-1}), which allow us to monitor changes of the heme absorption spectrum at a concentration that is a hundred times higher than those usually used for optical spectroscopy.

SAXS experiments

SAXS experiments were performed using two different synchrotron beamlines, namely the SAS beamline at the LNLS (National Synchrotron Light Laboratory, Campinas, Brazil) and the ID2 beamline at ESRF (European Synchrotron Radiation Facility, Grenoble, France). At LNLS, the scattering vector Q ranges (Q is the scattering vector modulus defined as $Q = 4\pi\sin\theta/\lambda$, being 2θ the scattering angle, and λ the x-ray wavelength) from 0.024 to 0.22 $\AA^{-1}$. At ESRF, the Q-range was 0.022 to 0.30 $\AA^{-1}$. Cyt-c samples were measured at room temperature in 1.5-mm glass capillaries at ESRF (1 mm at LNLS). To avoid radiation damage, the exposure time was 0.1 s/frame at ESRF (200 s/frame at LNLS), and a lead shutter was used to protect the sample from excess radiation within periods where no data were recorded. The final scattering pattern was then averaged from at least 30 frames at ESRF (four frames at LNLS). The experimental intensities (radially averaged at ESRF) were corrected for background, buffer contributions, detector inhomogeneities, and sample transmission. The scattering cross-sections have been converted to absolute units (cm^{-1}) by calibration with lupolen.

Data analysis

Basic equations

The small angle scattering of x-ray (or neutrons) is a powerful tool that yields information on the overall shape and size of biological macromolecules in solution. Its application is thus particularly useful in studying systems where large structural or conformational changes take place, like processes of protein folding/unfolding (Trewhella, 1997; Kataoka et al., 1993, 1995; Pollack et al., 1999; Pérez et al., 2001 and reference therein). In the frame of the so-called two phase model, monodisperse proteins in a diluted solution (in the order of 10^{-5} M) act as randomly oriented scattering particles of homogeneous electron density ρ, dispersed in a solvent with different homogeneous electron density ρ_s (Guinier and Fournet, 1955). In this condition, the excess x-ray scattering intensity reduces to

$$I(Q) = c(\Delta\rho)^2 V^2 P(Q) S_M(Q) \tag{1}$$

in which c is the molar protein concentration, $\Delta\rho = \rho - \rho_s$ is the contrast, and V is the protein volume. $P(Q)$ is the averaged squared form factor, which contains information on the size and shape of the protein molecule. $S_M(Q)$ is the structure factor based on the interference between waves scattered by different proteins. Its effect can be neglected ($S_M(Q) \cong 1$) for diluted solutions. An isotropic Fourier transform connects the form factor $P(Q)$ to the distance distribution function $p(r)$, the probability of finding pair of small volume elements at a distance r within the entire volume of protein,

$$P(Q) = \int_0^\infty p(r)\,\frac{\sin(Qr)}{Qr}\,dr$$

$$\Leftrightarrow p(r) = \frac{2r}{\pi}\int_0^\infty P(Q)Q\sin(Qr)dQ \tag{2}$$

The behavior of $I(Q)$ at small Q is approximated by the Guinier law (Guinier and Fournet, 1955)

$$I(Q) \cong I(0)\exp(-R_g^2 Q^2/3) \tag{3}$$

in which R_g is the gyration radius, defined for a homogeneous scattering particle by

$$R_g^2 = \frac{1}{2}\int_0^\infty r^2 p(r)dr \tag{4}$$

and

$$I(0) = c(\Delta\rho)^2 V^2 \quad (5)$$

is the scattering intensity at zero angle. For globular proteins, the Guinier approximation is strictly valid only for $QR_g \leq 1.3$ (Feigin and Svergun, 1987). It should be observed that R_g and $I(0)$ are respectively related to the average dimension of the protein and to the concentration of the scattering particles. In the case of aggregation, for monodisperse scattering particles constituted by n monomers of volume (V), the Eq. 5 transforms to

$$I(0) = nc(\Delta\rho)^2 V^2. \quad (6)$$

Under the assumption of monodispersity, from the Guinier analysis it is then possible to determine the aggregation state of the protein.

In the paper, we will made an extensive use of Kratky plots (i.e., $Q^2 I(Q)$ versus Q plot) to show the scattering data. The Kratky plot is indeed a useful tool in SAXS analysis for the characterization of globular protein and for the detection of intermediate folded states (Kataoka et al., 1993, 1995; Semisotnov et al., 1996). For a globular particle, the Kratky plot shows a typical peak, whose position mainly depends on its gyration radius R_g. On the other hand, when an unfolding process takes place, the peak usually vanishes and the curve tends to show a plateau when the protein assumes a completely unfolded random-coil conformation.

Concerning the $p(r)$ function, which contains direct information on the protein structure, it should be observed that it can be calculated from the experimental $I(Q)$ through the Eq. 2 only in a few cases, due to the limitation of the accessible Q range. Therefore, to reconstruct the shape of the scattering particles, different procedures should be adopted, usually based on the comparison of the form factor of refined model shapes to the experimentally observed scattering intensity. The different method used in this work are summarized below.

Monte Carlo form factor for globular protein

When the crystallographic structure of a protein is known, the distance distribution functions $p(r)$ of the protein can be calculated using Monte Carlo methods (Hansen, 1990; Henderson, 1996; Ashton et al., 1997; Svergun, 1997; Mariani et al., 2000). According to Mariani and coworkers (2000), the scattering particle can be described by the $s(\mathbf{r})$ function, which gives the probability that the point $r \equiv (r, \omega_r)$ (in which ω_r indicates the polar angles α_r and β_r) lies within the particle. For a compact particle (Stuhrmann et al., 1977), the $s(\mathbf{r})$ function can be written in terms of a unique two-dimensional angular shape function $\mathcal{F}(\omega_r)$, as

$$s(\mathbf{r}) = \begin{cases} 1 & r \leq \mathcal{F}(\omega_r) \\ \exp\{-[r - \mathcal{F}(\omega_r)]^2/2\sigma^2\} & r > \mathcal{F}(\omega_r) \end{cases} \quad (7)$$

in which σ is the width of the Gaussian that accounts for the effect of the chain mobility on the protein surface or/and to the presence of a hydration shell with density (and then electron density) different from the density of the bulk water (Svergun et al., 1998). The function $\mathcal{F}(\omega_r)$ is evaluated from the envelope surface of the van der Waals spheres placed in the crystallographic coordinates. The $p(r)$ histogram is then calculated taking into account the distances between all pairs of M points randomly generated and evaluated according to Eq. 7. The Monte Carlo form factor is then calculated by the Eq. 2.

For the native cyt-c, we used the high-resolution nuclear magnetic resonance and restrained simulated annealing structure reported by Banci and co-workers (1999) and deposited in the protein data bank (http://www.rcsb.org/pdb/) with the entry code 1GIW. The $p(r)$ functions obtained using $M = 5000$ and $\sigma = 0$ (dry protein) and $\sigma = 1.3$ Å (hydrated protein, see below) are reported in Fig. 4 (see below). The corresponding radii of gyration, calculated using Eq. 4, were 12.6 and 13.8 Å, respectively, whereas the protein volumes, determined by the ratio between the accepted and the total number of Monte Carlo moves were 13,900 and 18,600 Å^3, respectively.

Model form factors for unfolded protein

The low-resolution structure of unfolded or partially folded states of a protein is quite a tough problem, which cannot be tackle with a model-independent approach. In most cases, denatured proteins are a collection of different conformers where the secondary structure is approximately conserved. In the case of a completely unfolded chain, a suitable model to be applied is the Debye one (Debye, 1947), which is a flexible chain with a random walk-like conformation (random-coil chain). In this model, the distribution of the scattering centers in the real space follows a Gaussian statistics. The corresponding form factor is given by

$$P_{\mathrm{Debye}}(Q) = 2[\exp(-R_g^2 Q^2) + R_g^2 Q^2 - 1]/(R_g^2 Q^2)^2 \quad (8)$$

with $R_g^2 = Lb/6$. b is the statistical segment (Kuhn) length, representing the separation between two adjacent scattering centers, and L is the contour length, a measure of the chain length. It should be observed that to derive the R_g value, the Guinier approximation (Eq. 3) should be used in the usual Q-range for proteins in rather globular states only, whereas for unfolded proteins the Debye equation should be preferred (for example, see Pérez et al., 2001).

More physical models describing semiflexible or worm-like polymers have been developed. A detailed analysis has been recently published by Pedersen and Schurtenberger (1996). They report a Monte Carlo simulation study of the worm-like chain model of Kratky and Porod (1949), both considering the presence or the absence of excluded volume effects. Results are given in terms of approximated analytical expressions, which have been parametrized to reproduce SAXS scattering profiles. In particular, in the absence of excluded volume effects, the worm-like chain form factor, regardless of the cross-section contribution, can be determined by

$$\begin{aligned} P_1(Q) = \Bigg\{ & 2[\exp(-R_g^2 Q^2) + R_g^2 Q^2 - 1]/(R_g^2 Q^2)^2 \\ & + \left[\frac{4}{15} + \frac{7}{15 R_g^2 Q^2} - \left(\frac{11}{15} + \frac{7}{15 R_g^2 Q^2}\right)\exp(-R_g^2 Q^2)\right]\frac{b}{L}\Bigg\} \\ & \times \exp[-((Qb)/q_1)^{p_1}] + \left(\frac{1}{LbQ^2} + \frac{\pi}{LQ}\right) \\ & \times (1 - \exp[-((Qb)/q_1)^{p_1}]) \end{aligned} \quad (9)$$

when $L/b > 2$, and by

$$\begin{aligned} P_2(Q) = \{ & 2[\exp(-\langle R_g^2\rangle_0 Q^2) + \langle R_g^2\rangle_0 Q^2 - 1]/(\langle R_g^2\rangle_0 Q^2)^2\} \\ & \times \exp[-((Qb)/q_2)^{p_2}] + \left(\frac{a_1}{LbQ^2} + \frac{\pi}{LQ}\right) \\ & \times (1 - \exp[-((Qb)/q_2)^{p_2}]) \end{aligned} \quad (10)$$

with

$$\langle R_g^2\rangle_0 = \frac{Lb}{6}\left(1 - \frac{3}{2n_b} + \frac{3}{2n_b^2} - \frac{3}{4n_b^3}[1 - \exp(-2n_b)]\right) \quad (11)$$

and $n_b = L/b$ when $L/b \leq 2$. The optimum parameter values are $q_1 = 5.53$, $p_1 = 5.33$, $a_1 = 0.0625$, $p_2 = 3.95$, $a_2 = 11.7$, and $q_2 = a_2/L$, as shown in Pedersen and Schurtenberger (1996). In the case of finite section of the chains, the form factors described by Eqs. 8 (random-coil chain) and 9 and 10 (worm-like chain) should be multiplied for the form factor of the cross-section $S_{sc}(Q)$. The simplest approximation is to assume a local cylindrical shape, which reads $S_{sc}(Q) = [2J_1(RQ)/(RQ)]^2$, being $J_1(RQ)$ the first order Bessel function and R the cross-section radius.

Protein shape reconstruction from the multipole expansion method

In the case of monodisperse diluted protein, a well-established method for particle shape reconstruction is based on the expansion in series of spherical harmonics of the shape function,

$$\mathcal{F}(\omega_r) = \sum_{k=0}^{K} \sum_{m=-k}^{k} f_{k,m} Y_{k,m}(\omega_r). \tag{12}$$

Here K denotes the maximal rank of the spherical harmonics $Y_{k,m}(\omega_r)$ (Svergun and Stuhrmann, 1991). Recently this method was improved, introducing the group theory and the maximal entropy to deduce in a more efficient way the shape of the scattering particles (Spinozzi et al., 1998). The idea was to introduce the particle symmetry by considering its point group $\mathcal{G}$, and then to explore the fitting parameter space using a sequence of decreasing symmetries. The resulting symmetryzed shape function is

$$\mathcal{F}^S(\omega_r) = \exp\left\{ \sum_{k=0}^{K} \sum_{m=-k}^{k} a_{k,m} Y^S_{k,m}(\omega_r) \right\} \tag{13}$$

in which the symmetry spherical harmonics $Y^S_{k,m}(\omega_r)$ are compatible with the group $\mathcal{G}$ and $\{a_{k,m}\}$ is a set of parameters that can be determined to fit the experimental scattering curve. The finally recovered shape is the best compromise between a simple and hence symmetrical shape, i.e., a shape described by few parameters, and a good agreement with the experimental data.

Data fitting

In all cases, the analysis of the experimental curves $I(Q)$ of N_Q points has been performed by minimizing the reduced chi squared:

$$\chi^2 = \frac{1}{N_Q - N_P} \sum_{i=1}^{N_Q} \left[\frac{I(Q_i) - \kappa P(Q_i)}{\delta_i} \right]^2 \tag{14}$$

in which $P(Q)$ is the fitting form factor, κ is a scaling factor corresponding to the fitted scattering intensity at $Q = 0$ (see Eq. 15), δ_i is the experimental uncertainty of the scattering curve at the point Q_i, and N_P is the number of fitting parameters.

Estimate of the protein tertiary structure from the shape function: the filling approach

If a relevant part of the secondary structure of a protein is known, it can be useful to have a method that allows an estimate of the tertiary structure compatible with the reconstructed two-dimensional shape function $\mathcal{F}(\omega_r)$. Here we propose a simple algorithm to accomplish this task. The N_S secondary structure elements, namely α-helix or β-sheet domains, are separated by random coil sequences, which can be thought of as hinge elements. Due to the low resolution of the SAXS technique, it is useless to describe in detail all conformational changes of the random sequences, but it can be a reasonable simplification to leave fixed their structure except a free rotation around the C_α atom in the middle of the sequence. In this way, the protein conformational degrees of freedom are simply reduced to rotations (typically described by three Euler angles) around those hinges. A tertiary structure will be defined by the $N_S - 1$ sets of three Euler angles, $\{\omega_h^{(k)} \equiv (\alpha_h^{(k)}, \gamma_h^{(k)})\}$, which give the orientation of the k-th domain with respect the $(k - 1)$-th. Moreover, the space configuration of the whole protein will be determined by the translation vector, $\mathbf{R}_P$, of its mass center and by the Euler angles, ω_P, describing its overall orientation. In the case of protein aggregates (e.g., a dimer), we need of more translational and orientational coordinates for describing the mutual position between single monomers. That tertiary structure where the largest number of atoms are contained in the volume enclosed by the SAS-reconstructed shape will be the best estimate compatible with the experimental data. The "best filling" conformation can thus be calculated by minimizing the root mean square (*rms*)

$$\text{rms} = \left[V - \sum_{i=1}^{N_A} s(\mathbf{r}_i) V_i^{(\text{vdW})} \right]^2 \tag{15}$$

in which, V is the protein volume, N_A the number of atoms, $s(\mathbf{r})$ the position function (Eq. 7), $V_i^{(\text{vdW})}$ the van der Waals volume of the i-th atom, and $\mathbf{r}_i$ its position, which is a function of the configurational variables $\mathbf{R}_P$, ω_P, $\{\omega_h^{(k)}\}$. Here $s(\mathbf{r}_i)$ plays the role of a filter function, which discards the i-th atom if it is not inside the shape. The configurational variables are optimized by using a Monte Carlo trial and error procedure.

It is worth notice that the filling method is here used only to test if the reconstructed shape fits with the mean dimensions of the cyt-c structure elements. Any attempt to derive the real tertiary structure from SAXS data by using this approach falls outside the aim of this work and will be the object of a specific paper.

RESULTS AND DISCUSSIONS

Optical absorption measurements

Acidification of a salt-free solution of cyt-c using HCl leads to an increase of the absorbance peak at 620 nm, characteristic of high-spin complexes. Optical spectra of cyt-c show the presence of two subsequent transitions with increasing the HCl concentration (Fig. 1). The first transition is ascribed to $N \rightarrow U_1$ and the second to $U_1 \rightarrow A_1$ state. The former is a cooperative transition, which occurs at [HCl] = 14 mM for 0.8 mM concentration of protein. The latter can be obtained by further addition of HCl. The presence of these two transitions, when the protein is titrated in absence of salt, is a well-documented behavior of the cit-c (Ohgushi and Wada, 1983; Weber et al., 1987; Goto et al., 1990a; Fink et al., 1994). As previously shown (Boffi et al., 2001), the two transitions are well resolved at [cyt-c] = 0.8 mM, whereas they partially overlap at higher concentrations. This fixes a limit to the protein concentration that can be used in SAXS measurements to characterize the U_1 state. In fact, at high protein concentration, upon decreasing the pH, the protein will go directly into A_1 state from the N state.

The addition of NaCl to the protein in the U_1 state also leads to a collapse into a partially refolded intermediate state (A_2) (Goto et al., 1990a,b). The principal responsible for the refolding is thought to be the binding of chloride anions. In fact, they minimize the intramolecular charge repulsion that initially caused the protein unfolding. However, as shown in Fig. 1, the $\Delta\epsilon$ at 620 nm of the NaCl induced state A_2 is larger than that of HCl induced one,

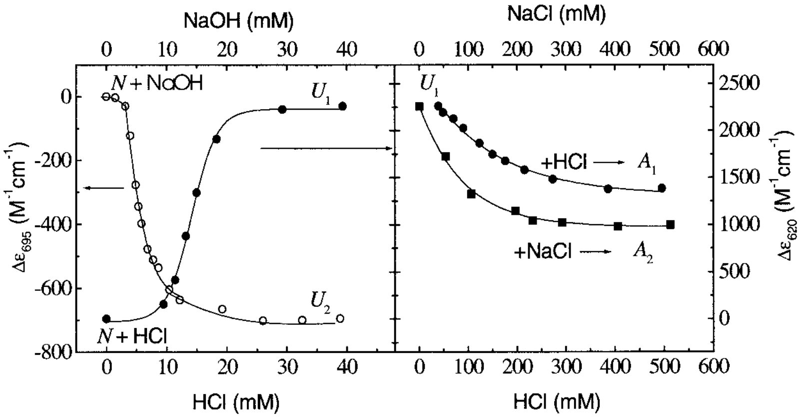

FIGURE 1 Changes in extinction coefficients at 695 nm (λ) and at 620 nm (μ, ν) as a function of the concentration of NaOH (λ), HCl (μ), and NaCl at pH 2(ν). The size of the symbol is representative of the error. Lines are guide for eyes.

indicating that some differences between A_1 and A_2 conformations should occur. This may reflect the difference in heme iron local structure indicated by XAS measurements (Boffi et al., 2001).

In the alkaline-unfolded U_2 state, the absorption band of cyt-c at 695 nm is absent; the complete disappearing of this band indicates that protein looses the methionine-80 as sixth ligand to the Fe heme. The dependence on NaOH concentration of the protein extinction coefficient at 695 nm is also shown in Fig. 1. In this case the cyt-c unfolds in a single cooperative transition around [NaOH] = 5 mM, assuming the U_2 unfolded state at [NaOH] = 30 mM.

SAXS measurements

SAXS experiments have been performed on cyt-c solutions at low ionic strength at different pH (pH 7 in the native conformation N; pH 2 in the fully acid-unfolded state U_1; pH 12 in the fully alkaline-unfolded state U_2) and further decreasing the pH from 2 to 0.5 using HCl (to obtain the A_1 state) or increasing the ionic strength at constant acidic pH from 0 to 500 mM using NaCl (to obtain the A_2 state). Examples of the experimental SAXS profiles obtained in the different investigated conditions are reported in the Fig. 2 in the form of Kratky plots.

The radii of gyration and the intensities scattered at Q = 0 have been obtained by using both Guinier and Debye laws (Eqs. 3 and 8). However, only the Guinier results are reported for the following reasons: 1) the Kratky plots show the presence of a more or less pronunced peak and 2) the conclusions reached in this work (see next sections) give an indication that a rather high degree of globularity is preserved in the investigated cyt-c states. The fitting results are then shown in Fig. 3 and Table 1. It should be first observed that the R_g do not show a significant trend with protein concentration, indicating that interaction effects can be disregarded, i.e., the obtained parameters can be equated to the actual structural characteristics of the cyt-c in the different stable states. Moreover, it can be noticed that the radii of gyration of the alkaline unfolded state (U_2) and of the molten globule intermediate induced adding NaCl at pH 2 (A_2 form) are rather similar to that of the native protein (N). By contrast, larger R_gs are observed both for the acidic unfolded state (U_1) and for the acid-recompacted state (A_1). These experimental data can be compared with the radius of gyration of the cyt-c determined from the crystallographic coordinates (Banci et al., 1999), $R_{g,th}$ = 12.6 Å. Whereas the small variations could be related to changes in the hydration properties of the protein surface or to small conformational adjustments induced by solvent effects, the large radius of gyration observed at very low pH (U_1 and A_1) strongly suggests the occurrence of large conformational changes or the formation of protein aggregates. From this point of view, it should be observed that a radius of gyration of 32.4 (±1.6) Å has been reported by Kataoka and co-workers (1993) for the cyt-c in 4 M guanidine-HCl, which is thought to fully unfold the protein.

According to the Eq. 6, information on the protein aggregation properties can be directly obtained from the scattered intensity at zero angle. Assuming that the solution is monodisperse and using for the cyt-c the molecular volume of 18,600 Å^3 (see above) and the electron density contrast calculated in the different experimental conditions from the solution chemical composition (namely, taking into account the presence of salts and counter-ions), the aggregation numbers n in Table 1 have been determined. In particular, the presence of dimer is strongly suggested for the A_1 state. However, molecular information can be hardly derived from these parameters. Further structural information has been then obtained, applying the different approaches above described (see Materials and Methods) to analyze the SAXS curves. The results are reported in the following paragraphs in which the different cyt-c states are separately analyzed.

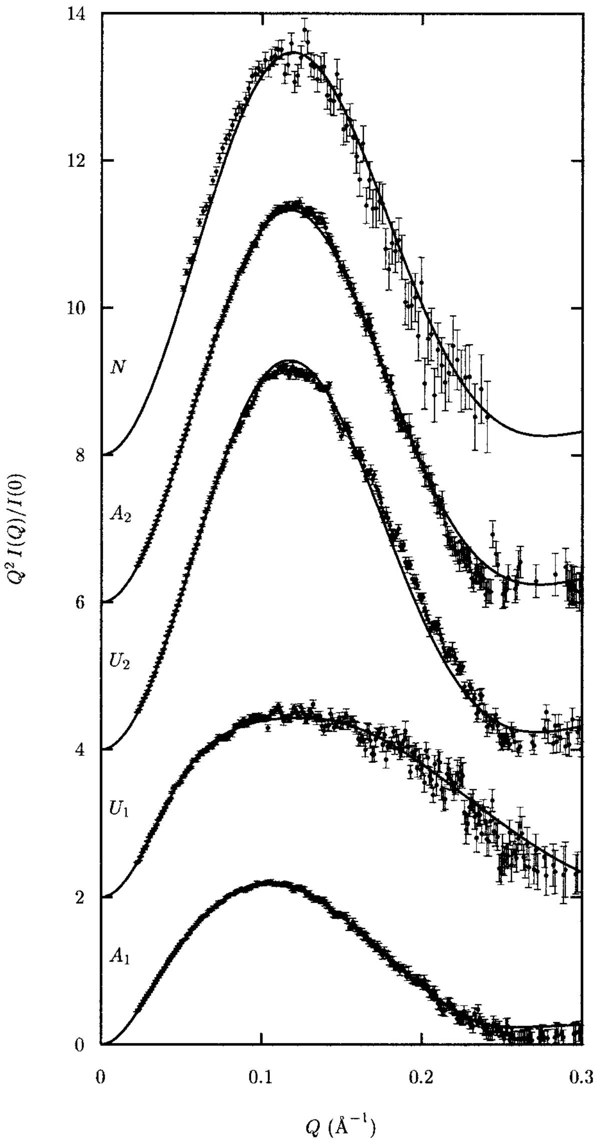

FIGURE 2 SAXS profiles obtained from cyt-c at concentration 0.8 mM in native (N), acid-denatured (U_1), acid-induced recompacted (A_1), salt-induced recompacted (A_2), and alkaline-denatured (U_2) states. All curves were measured at ESRF, beamline ID02, except the native sample, which was measured at the SAXS beamline of LNLS. The curves are in the form of Kratky plots and are normalized for the $I(0)$ values obtained by applying the Guinier law (Table 1) and scaled by a factor 2 for clarity. The solid curves correspond to the fits obtained by using the Monte Carlo method (N, A_1, U_2), the worm-like model (U_1), and the multipole expansion method (A_2), as described in the text.

Native N *state*

The SAXS results obtained at pH 7 have been analyzed by fitting the experimental curve with the cyt-c crystallographic structure (Banci et al., 1999). However, because SAXS data indicate the presence of scattering particles with a radius of gyration larger than that estimated from the atomic coordinates, the presence of a border shell around the protein, attributed to the mobility of the chains on the protein surface or/and to the presence of a hydration shell, has been taken into account (Svergun et al., 1998).

The calculated scattering intensity (in the form of Kratky plot) and the best fit parameters are reported in Fig. 2 and Table 2, respectively. From the figure, the quality of the fit can be directly appreciated: it is interesting to note that the width of the Gaussian that accounts for the particle border, σ, is 1.3 Å, in agreement with data obtained for other globular proteins (Svergun et al., 1998; Baldini et al., 1999). The corresponding scattering particle volume, as determined using the Monte Carlo procedure described by Mariani and co-workers (2000), is 18,600 Å^3, in perfect agreement with the particle volume that can be determined from the calculated scattering curve from the Porod invariant $V = 2\pi^2/\int_0^\infty P(Q)Q^2 dQ$ (Guinier and Fournet, 1955).

For the sake of completeness, the distance distribution function $p(r)$ and the three-dimensional structure of the N cyt-c are also reported in Figs. 4 and 5, respectively. The unimodal shape of the $p(r)$ function confirms the globular and compact nature of the protein in the native conformation. It should be observed that the largest dimension of the protein is ~40 Å.

Acid-denatured U_1 *state*

At the neutral pH, cyt-c is a globular protein having two strong-field ligands to the heme iron, an imidazole nitrogen of His-18 and a sulfur of Met-80, coordinated in axial positions of the heme plane. When titrated with HCl in absence of salt (Fig. 1), the optical spectra of the protein show a first transition at pH near 3, resulting in the unfolded state U_1, where the heme axial ligand is probably lost. Indeed, in agreement with the undefined nature of the sixth ligand (Scott and Mauk, 1996), the XANES spectrum presents characteristics of a met-myoglobin at pH 4 (Boffi et al., 2001).

The present SAXS measurements confirm significant differences between the native N and the acid-denatured U_1 states. If the radii of gyration are very different (see Table 1), the clear peak detected in the Kratky plot appears larger than that observed in the native state and less steep at higher Q (compare in Fig. 2). The presence of a peak in the Kratky plot is a clear indication that the protein state is sufficiently globular, because the curve for an expanded unfolded conformation is expected to show a plateau and then to increase monotonically (Kataoka et al., 1993, 1995; Semisotnov et al., 1996). However, this is strictly valid only for an infinitely thin, random coil polymer, and the Kratky plot of a random coil polymer with a finite section could be undistinguishable from that of a protein in a globular state. To derive the conformational state of the acid-denatured form of cyt-c, the SAXS curve has been then tentatively fitted considering different models. As illustrated in Fig. 6, poor fitting results (in particular at high Q values) were obtained

TABLE 1 Radii of gyration and forward scattering intensities calculated by applying the Guinier approximation (Eq. 3) to SAXS data from cyt-c in the native (*N*), acid-denatured (U_1), acid-induced recompacted (A_1), salt-induced recompacted (A_2), and alkaline-denatured (U_2) states

State	pH	c (mM)	[HCl] (mM)	[NaCl] (mM)	[NaOH] (mM)	R_g (Å)	$I(0)$ (cm^{-1})	n	Beamline
N	7	0.79	–	–	–	13.8 ± 0.4	0.150 ± 0.002	1.1	LNLS
		0.59	–	–	–	13.8 ± 0.2	0.123 ± 0.004	0.9	LNLS
		0.39	–	–	–	14.3 ± 0.7	0.070 ± 0.008	1.0	LNLS
U_1	2	0.78	42	–	–	24.0 ± 0.2	0.146 ± 0.007	1.1	ESRF
		0.61	31	–	–	25.6 ± 0.3	0.103 ± 0.008	1.0	ESRF
		0.40	27	–	–	24.7 ± 0.8	0.082 ± 0.005	0.9	LNLS
U_2	12	0.82	–	–	30	14.8 ± 0.1	0.130 ± 0.001	0.9	ESRF
		0.64	–	–	30	14.7 ± 0.1	0.112 ± 0.002	1.0	ESRF
		0.42	–	–	30	14.9 ± 0.1	0.063 ± 0.004	0.9	ESRF
A_1	0.5	0.85	450	–	–	26.7 ± 0.2	0.261 ± 0.005	1.9	ESRF
		0.66	450	–	–	27.8 ± 0.3	0.225 ± 0.008	2.1	ESRF
		0.44	450	–	–	25.7 ± 0.2	0.127 ± 0.009	1.8	LNLS
A_2	2	0.85	43	450	–	14.5 ± 0.1	0.151 ± 0.001	1.1	ESRF
		0.66	31	450	–	14.1 ± 0.1	0.130 ± 0.003	1.2	ESRF
		0.40	27	450	–	14.2 ± 0.1	0.067 ± 0.006	1.0	ESRF

using Eq. 8, also considering a finite section of the random-coil chain (Fig. 6 *c*) or assuming the presence in solution of a mixture of cyt-c in the native conformation and in a fully unfolded state, as described by the Debye model (Fig. 6 *d*). Bad results were also obtained by analyzing the SAXS experimental curve with the multipole expansion method, which is based on the presence of compact and globular-like particles (Spinozzi et al., 1998). On the other hand, good fit to the data was obtained using the scattering model for semiflexible worm-like polymers (see Eqs. 9 and 10) (Figs. 2 and 6 *a*). The parameters that describe the chain are the radius of the finite cylindrical cross-section, R, the contour length, L, and the statistical segment length, b, which is a measure of the flexibility of the chain. The best-fit parameters are reported in Table 2, whereas the corresponding $p(r)$ function is shown in Fig. 4.

Therefore, to derive the structural model, five relevant points need to be resumed: 1) the aggregation number n (Table 1), derived assuming a monodisperse solution, indicates that the protein is monomeric; 2) the Kratky plot is uncompatible with an expanded fully unfolded conformation of the protein (random-coil conformation), but it is also proving the absence of globular-like particles; 3) the worm-like chain model fits well the experimental data; 4) the L/b ratio (which corresponds to the number of chain element in the whole chain) is around 2 (see Table 2). It should be noticed that in polypeptides, L/b can be regarded as the number of structural subunits or segments of the polymer that appears to behave randomly, and b is the effective length of these random segments (Van Holde et al., 1998). The fitted b value is 55 Å (see Table 2); 5) the distance distribution function (see Fig. 4) shows a bimodal nature and indicates that the largest dimension of the scattering particle is ~90 Å. Therefore, we suggest a two-domain structure for the acid-denatured U_1 state of cyt-c; the two subunits, which should be characterized by a some degree of order, are 55 Å long. As a confirmation, simulations based on a very simple bimodal structural model made by two compact subunits flexibly jointed end-to-end and with randomly distributed bond angles have been performed. A very good fit to the scattering data was obtained using cylindrical subunits of 55 Å height and 11.5 Å radius, in good agreement with the worm-like model parameters (Fig. 6 *b*). The scattering curve obtained from the two-cylinder model is reported in Fig. 2, whereas the particle model is sketched in Fig. 5.

Because of the detected partial compactness of the subunits, it could be suggested that during unfolding two protein domains, which retain some degree of the secondary structure, move apart, rotating around regions of unfolded polypeptide chain. This process is consistent with the loss and/or the change of the heme axial ligand detected by XAS (Boffi et al., 2001). Because the two larger N- and C-terminal α-helices of cyt-c are stable in acidic conditions (Jeng et al., 1990), and because their dimensions compare with the height of the cylindrical subunits, each protein domain may be essentially constituted by one of the α-helices. The filling procedure gave rise to the picture sketched in the Fig. 5: the first cylinder is filled by the amino acids forming the larger N-terminal α-helix, the successive short α-helix, and the heme group bound to the His-18; the other cylinder is in turn filled by the amino acids forming the C-terminal α-helix and the pair of remaining short α-helices (where the Met-80 is located). Nevertheless, it should be observed that the geometrical volume of the bimodal structure is two times larger that the nominal protein volume, suggesting that the amount of secondary structure is much lower than that indicated in the model picture and that the exposure of unfolded polypeptide regions is accomplished through

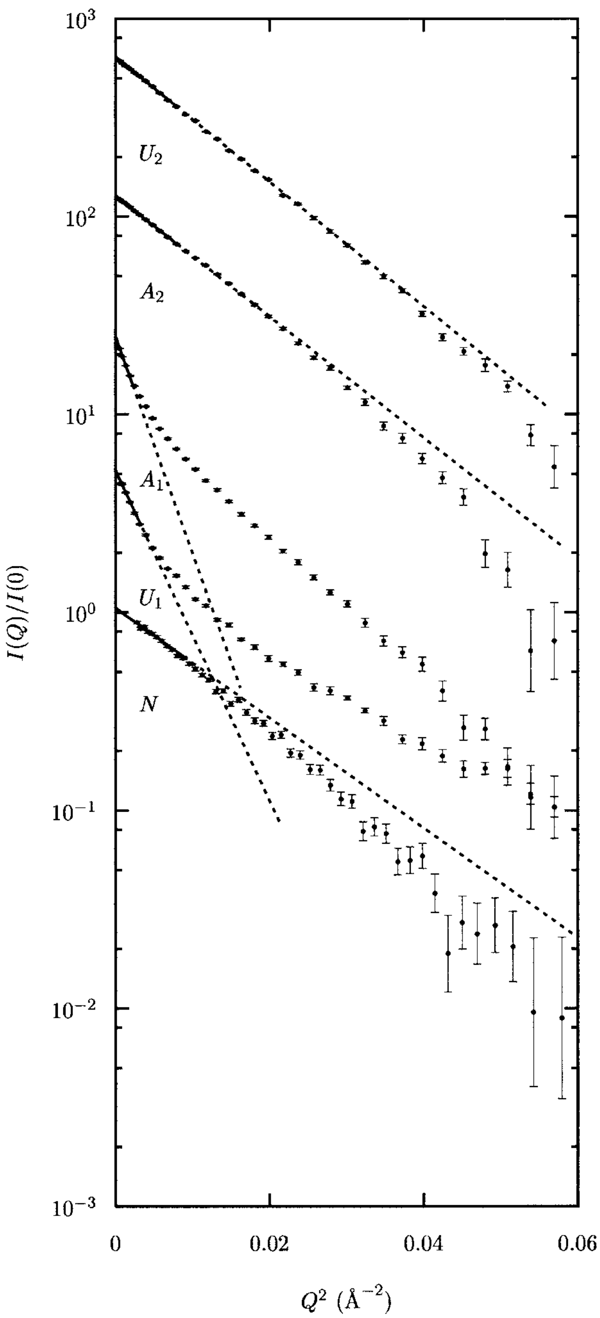

FIGURE 3 Guinier plots of SAXS data obtained from cyt-c at concentration 0.8 mM in the native (N), acid-denatured (U_1), acid-induced recompacted (A_1), salt-induced recompacted (A_2), and alkaline-denatured (U_2) states. The curves are normalized for the $I(0)$ values obtained by applying the Guinier law (Table 1) and scaled by a factor 5 for clarity. The solid lines correspond to the fits obtained by using the Guinier law.

favorable water interactions. Therefore, experimental data are consistent with the indication that acid denaturation of proteins results in states that are less unfolded than those obtained with high concentrations of urea or guanidinium chloride (Tanford, 1970; Fink, 1995).

Acid-induced recompacted A_1 *state*

Starting from the U_1 state, the addition of NaCl or HCl realizes the collapse into compacted intermediate states, indicating that the chloride anion should play a key role in these acid- or salt-induced transition to molten globule conformations. Acid-salt-induced transitions are a common phenomenon to several quite different proteins. Therefore, the general idea is that in the acidic denaturation, intramolecular charge repulsion is the driving force for unfolding. The shielding of intramolecular charge-charge repulsion forces in the U_1 state by anions brings to the formation of a molten globule state (Kataoka et al., 1993; Fink, 1995). However, in the present case, the recompacted states obtained after addition of NaCl and HCl show very different radii of gyrations and forward scattering intensities (see Table 1), suggesting a different structure or at least a different aggregation behavior, with the formation of dimeric particles in the case of the acid-induced recompacted state (A_1). Noticeable is that in both cases the Kratky plots (Fig. 2) indicate that the degree of compactness and globularity of the scattering particles is quite high.

The structural analysis of the acid-recompacted A_1 state has been performed both fitting the experimental curve with different protein models and reconstructing the shape of the scattering particles using the multipole approach. No satisfactory fits to the data have been obtained neither considering the worm-like model nor using globular and dumbbell dimeric models based on the crystallographic coordinates of cyt-c (also taking into account the hydration shell). Moreover, any attempt to fit the scattering curve using a combination of scattering functions related to these protein models has been unsatisfactory (Fig. 6 b'). Structural information has been then directly derived from the particle shape function reconstructed using the multipole approach. The best fit curve is shown in Figs. 2 and 6 a'.

The particle shape and the corresponding $p(r)$ function, which are reported in Figs. 5 and 4, respectively, are consistent with a dimeric compact structure. Considering that the volume of the reconstructed particle is more than two times larger that the volume of the native cyt-c (see Table 2), the formation of dimers appears clearly confirmed. From XAS measurements, it was derived that in the A_1 state the pentacoordinate heme with an imidazole as fifth ligand represents the best model to fit the local environment of the heme iron. Moreover, recent kinetic studies of the refolding of cyt-c (Pollack et al., 1999) have demonstrated that the molten globule-like intermediate can be trapped because of the presence of non-native His coordination (His-26 or His-33). The axial ligand, although non-native, increases the stability of compact conformation. These results indicate that the native ligands are not necessarily required for the formation of compact states. However, the presence of non-native bonds can lead to the exposure of charged or hydrophobic surfaces that may determine association pro-

TABLE 2 Fitting results of SAXS curves from cyt-c in the native (*N*), acid-denatured (U_1), acid-induced recompacted (A_1), salt-induced recompacted (A_2), and alkaline-denatured (U_2) states

State	Method	χ^2	κ (cm^{-1})	V (10^3 Å^3)	Fitting parameter		
N	Monte Carlo	1.4	0.143	18.6	σ	1.3	Å
U_1	Worm-like	1.7	0.140	36.7	L	110.6	Å
					b	55.2	Å
					R	10.3	Å
U_2	Monte Carlo	0.9	0.127	23.9	σ	1.5	Å
A_1	Multipole expansion	1.3	0.264	48.6	$\mathcal{G}$	$\mathcal{C}_2$	
					K	5	
					N_P	18	
A_2	Monte Carlo	1.4	0.148	19.2	σ	2.3	Å

cesses increasing ionic strength. The comparison of the particle shape and dimensions with data relative to the U_1 state suggests a model in which aggregate formation occurs by the specific association of partially folded domains of cyt-c, which associate preferentially in an intermolecular fashion to form dimers, as opposed to intramolecular association leading to the native conformation. One of the possible dimer conformations, obtained by the Monte Carlo filling procedure under the assumption that the cyt-c have secondary but no tertiary structure, is represented in Fig. 5. The quality of the shape-function filling is a good support to classify the A_1 state as partially folded intermediate, the general characteristics of which include substantial secondary structure, little tertiary structure, substantial compactness, and propensity to aggregation (Fink, 1995).

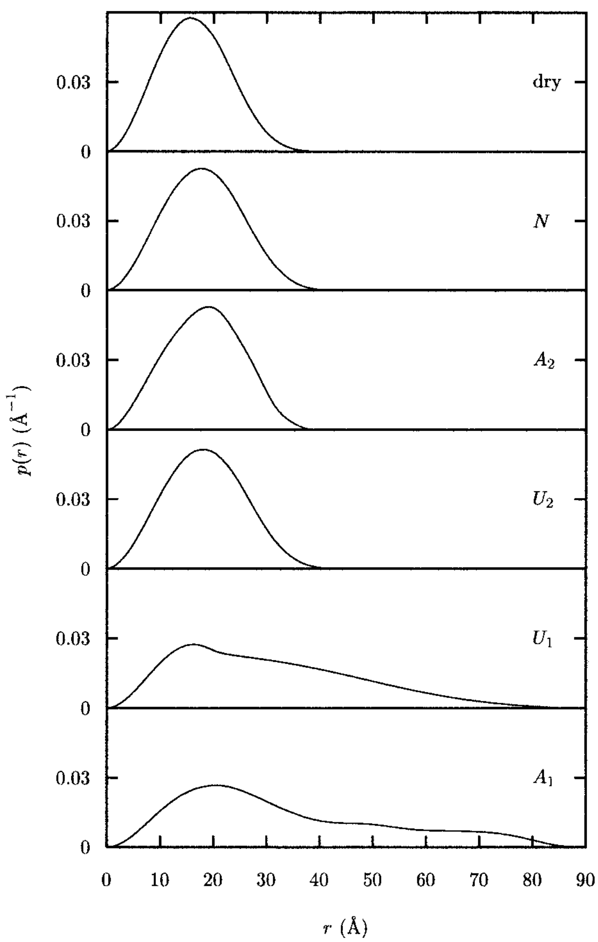

FIGURE 4 Distance distribution functions obtained from the crystallographic coordinates of cyt-*c* (dry) and by the analysis of SAXS data obtained in the native (N), acid-denatured (U_1), acid-induced recompacted (A_1), salt-induced recompacted (A_2), and alkaline-denatured (U_2) states. For the dry, N, A_2, and U_2 forms, the $p(r)$ curves have been calculated by the Monte Carlo method with a variance σ of the Gaussian border shell of 0, 1.3, 1.5, and 2.3 Å, respectively; for the U_1 and A_1 states, the $p(r)$ curves have been obtained by Fourier transforms (see Eq. 2) of the corresponding fitting curves reported in Fig. 3.

Salt-induced recompacted A_2 *state*

From the unfolded state U_1, recompaction of cyt-c can be also induced by adding salt. The resulting state A_2 has a 5% larger radius of gyration than that of the native state (see Table 1), a difference similar to that already observed for other molten globul protein states (Kataoka et al., 1995). Moreover, the Kratky plot reported in Fig. 2 shows that the degree of compactness and packing density is very high, clearly indicating that the A_2 specie is as compact as the native state. Fitting procedure based on the crystallographic coordinates of the cyt-c showed that SAXS data can be very well reproduced by only adjusting the thickness of the hydration shell (see Fig. 2 and Table 2). According to the XAS experimental evidence that in this condition the heme local structure is very similar to that of the native state (Boffi et al., 2001), and to the CD analysis that indicate at pH 2 and in the presence of chlorine anions a significant presence of native-like secondary structure (Goto et al., 1990a and Fink et al., 1994), we suggest that the recompaction process, through favorable intramolecular interactions, realizes a globular and compact conformation. Noticeable is that the hydration shell obtained from the fitting procedure has a σ of 2.3 Å, larger than that observed in the native state (σ = 1.3 Å). This difference confirms that the conformation of the salt-recompacted state is more expanded than that of the native state, in agreement with the hypothesis that molten globules have a fluctuating tertiary structure. It is inter-

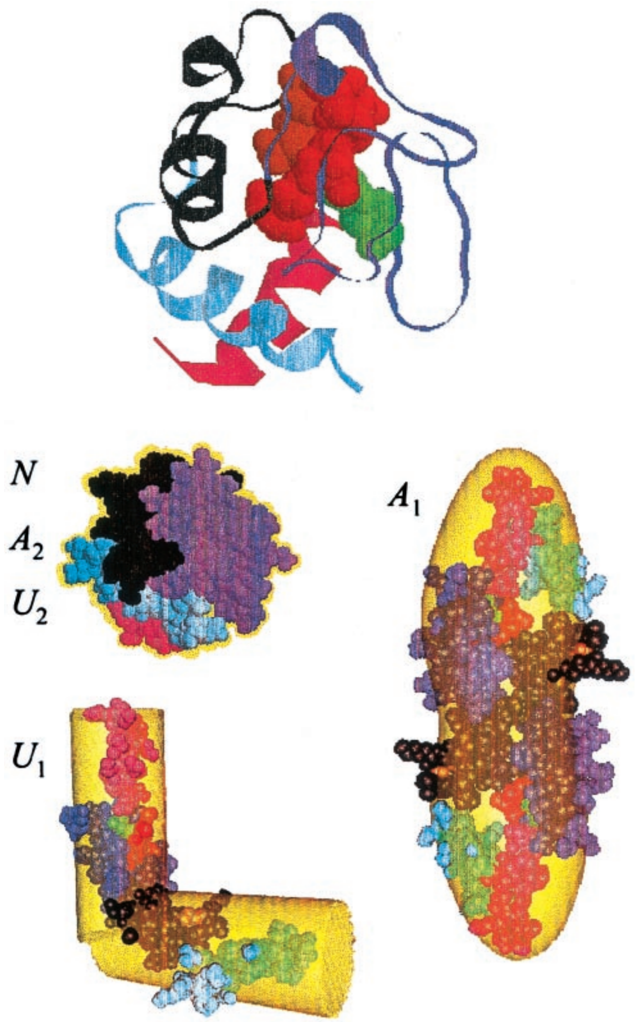

FIGURE 5 Three-dimensional representations of the structure of cyt-c in the native (N), acid-denatured (U_1), acid-induced recompacted (A_1), salt-induced recompacted (A_2), and alkaline-denatured (U_2) states, as resulting from the analysis of the corresponding SAXS data. (*Top*) View of the cyt-c, PDB code 1GIW (Banci et al. 1999), using RasMol 2.6 package (www.umass.edu/microbio/rasmol) with the "strands" option. The sequence of the 104 amino acids is represented in different colors corresponding to four regions of secondary structure: 1 to 16 (*magenta*) contains the large N-terminal α-helix; 17 to 57 (*blue*) includes the subsequent short α-helix; 58 to 84 (*black*) contains the two other short α-helices; 85 to 104 (*cyan*) includes the large C-terminal α-helix. The heme group and the two bound amino acids His-18 and Met-80 are represented using the "spacefill" option and with colors red, green, and orange, respectively. (N, A_2, U_2) "Spacefill" representation of the 1GIW structure used to analyze SAXS data with the Monte Carlo method. The yellow border, corresponding to an indicative variance $\sigma = 3$ Å of the Gaussian that accounts for the expanded conformation detected in the different cases, is shown. (U_1) Sketch of a possible conformation of the worm-like model constituted by two cylindrical subunits (*yellow*). To best fill the entire volume, the 1GIW tertiary structure has been modified rotating the four regions of secondary structure around the three separating amino acids (see text). (A_1) Shape function, $\mathcal{F}(\omega_r)$ (*yellow*), obtained by the multipole expansion method. According to the C_2 symmetry of a dimer, two 1GIW structures with modified tertiary structures have been used to best fill the reconstructed shape. The symmetry center position and the opening angles have been chosen by the best filling procedure described in the text.

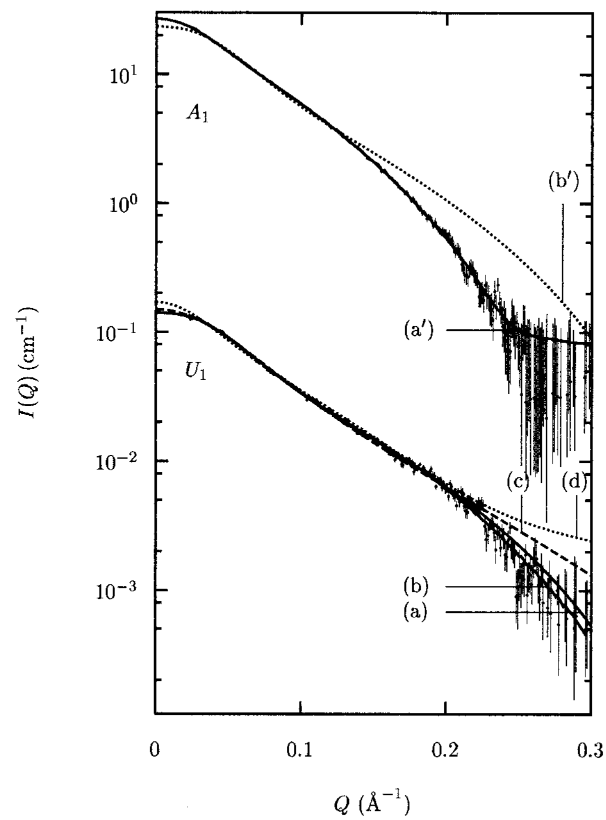

FIGURE 6 Comparison between different fitting models applied to the SAXS intensities from cyt-c in the acid-denatured (U_1) and acid-induced recompacted (A_1) forms. U_1 state: the curves correspond to the fits obtained using the worm-like model with a finite section (a), the Gaussian chain model with a finite section (b), the two cylinders flexibly jointed end-to-end model (c), a mixture between the native cyt-c form factor, and a Gaussian chain form factor (d). A_1 state (scaled by a factor 10^2 for clarity): fits obtained using the multipole expansion method (a') and a mixture between the native cyt-c form factor and the worm-like model form factor (b').

esting to observe that these characteristics fit the original definition by Ptitsyn for the molten globule state (Ptitsyn, 1987; Fink, 1995).

The whole results indicate that both the heme local and cyt-c global structures of the two acid- and salt-induced molten globule A_1 and A_2 states are completely different. Specific or nonspecific interactions both contribute to the stabilization the compact intermediate states. Because the anions concentration is the same, full protonation of protein residues or variations in the properties of the electrostatic shielding due to the nature of the added co-ions (Na^+ compared by H^+) appear to critically affect the final structure.

Alkaline-denatured U_2 *state*

The alkaline-denatured state of cyt-c, U_2, and the native N state have similar R_g values. Moreover, the peak observed in the Kratky plot reported in Fig. 2 indicates a globular structure. Accordingly, a good fit to the data has been obtained, calculating the scattering intensity from the crystallographic structure of cyt-c only adjusting the thickness of the border shell (see Table 2): it is interesting to note that the width of the border shell results comparable with that obtained form the native data. Finally, the Fig. 4 shows the $p(r)$ function, which confirms the globular and compact nature of the denatured state. All these results suggest that the cyt-c in the alkaline-denatured state has a compact conformation, although the small changes observed in both radius of gyration (~2%) and σ (~15%) could indicate that the mobility of the chains on the protein surface is increased with respect to the native structure.

Such results are in agreement with the small increase observed in the hydrodynamic radius by dielectric measurements (Scott and Mauk, 1996; Rossel et al., 1998) and the XAS evidence that the alkaline unfolded U_2 state is characterized by a six-coordinate, low-spin heme iron, which maintains the native imidazole ligand of His-18, whereas the sulfur atom of Met-80 is replaced by another strong-field ligand (Boffi et al., 2001). Therefore, the effect caused by basic pH consists in a partially unfolded process, which is mainly given by the displacement of the methionine S-iron linkage and by the occurrence of a stable structure packed as tightly as in the native state.

CONCLUSIONS

In solution, SAXS is provided to be a powerful technique for the characterization of the unfolded states of cyt-c. In particular, the full analysis of the scattering curves gives the possibility to characterize compactness, globularity, and aggregation properties of cyt-c in very different experimental conditions.

The first important implication is that the molten globule states A_1 (which forms at pH 2 from the acid unfolded state for addition of more acid) and A_2 (which forms at the same pH after addition of salt) show fairly compact structures. In good agreement with previous CD measurements (Goto et al., 1990a; Fink et al., 1990), these structures are compatible with the presence of large amounts of secondary structure. However, in agreement with the changes in heme binding detected by XAS measurements (Boffi et al., 2001), these two states are characterized by significant differences in globularity and aggregation properties. If a fluctuating tertiary structure could be responsible for the expanded conformation observed in the salt-recompacted A_2 state, intermolecular specific interactions, maybe involving hydrophobic or charged surfaces but sensitive to the effect of added co-ions, could stabilize the dimeric and substantially compact structure of the acid-induced A_1 state.

Concerning the structural property of the unfolded states, the alkaline-denatured U_2 form results surprisingly globular, whereas we suggest for the acid-unfolded U_1 form a two-domain expanded structure. Therefore, both states appear characterized by some degree of structure, in agreement with the indication that acid-denatured proteins posses a residual secondary structure (Tanford, 1970; Fink, 1995).

Much remains to be investigated, in particular for what concerns the fine balance of forces that determine the degree of folding and the stability of the different intermediates and the experimental evidence that the recompacted states are similar or identical to intermediates formed during the actual folding process. However, a final point should be stressed: the combined analysis of the local heme environment (obtained by XAS) and the global structure derived by a full analysis of the SAXS curves, allows us to extract the model structure for cyt-c in very different unfolding intermediates. This can be a good general way to derive systematic structural information on folding and unfolding processes for a number of proteins.

REFERENCES

Ashton, A. W., M. K. Boehm, J. R. Gallimore, M. B. Pepys, and S. J. Perkins. 1997. Pentameric and decameric structures in solution of serum amyloid P component by x-ray and neutron scattering and molecular modelling analyses. *J. Mol. Biol.* 272:408–422.

Baldini, G., S. Beretta, G. Chirico, H. Franz, E. Maccioni, P. Mariani, and F. Spinozzi. 1999. Salt induced association of β-lactoglobulin studied by salt light and x-ray scattering. *Macromolecules.* 32:6128–6138.

Banci, L., I. Bertini, J. G. Huber, G. A. Spyroulias, and P. Turano. 1999. Solution structure of reduced horse heart cytochrome c. *JBIC.* 4:21–31.

Boffi, F., A. Bonincontro, S. Cinelli, A. Congiu Castellano, A. De Francesco, S. Della Longa, M. Girasole, and G. Onori. 2001. pH-Dependent local structure of ferricytochrome c studied by x-ray absorption spectroscopy. *Biophys. J.* 80:1473–1479.

Christensen, H., and R. H. Pain. 1991. Molten globule intermediates and protein folding. *Eur. Biophys. J.* 19:221–229.

Debye, P. 1947. Molecular-weight determination by light scattering. *J. Physics Coll. Chem.* 51:18–32.

Döpner, S., P. Hildebrandt, F. I. Rossel, and A. G. Mauk. 1998. Alkaline conformational transitions of ferricytochrome c studied by resonance Raman spectroscopy. *J. Am. Chem. Soc.* 220:11246–11255.

Feigin, L. A., and D. I. Svergun. 1987. Structure Analysis by Small-Angle X-ray and Neutron Scattering. Plenum Press, New York.

Fink, A. L. 1995. Compact intermediate states in protein folding. *Ann. Rev. Biophys. Biomol. Struct.* 24:495–522.

Fink, A. L., L. J. Calciano, Y. Goto, T. Kurotsu, and D. R. Palleros. 1994. Classification of acid denaturation of protein: intermediates and unfolded states. *Biochemistry.* 33:12504–12511.

Goto, Y., L. J. Calciano, and A. L. Fink. 1990a. Acid induced folding of proteins. *Proc. Natl. Acad. Sci. U.S.A.* 87:573–577.

Goto, Y., N. Takahashi, and A. L. Fink. 1990b. Mechanism of acid-induced folding of proteins. *Biochemistry.* 29:3480–3488.

Guinier, A., and G. Fournet. 1955. Small angle scattering of X-ray. Wiley, New York.

Hansen, S. 1990. Calculation of small-angle scattering profiles using Monte Carlo simulation. *J. Appl. Crystallogr*. 23:344–346.

Henderson, S. J. 1996. Monte Carlo modelling of small-angle scattering data from non-interacting homogeneous and heterogeneous particles in solution. *Biophys. J.* 70:1618–1627.

Jacrot, B. 1976. The study of biological structures by neutron scattering from solution. *Rep. Prog. Phys.* 39:911–953.

Jacrot, B., and G. Zaccai. 1981. Determination of molecular weight by neutron scattering. *Biopolymers.* 20:2413–2426.

Jeng, M. F., S. W. Englander, G. A. Elöve, A. J. Wand, and H. Roder. 1990. Structural description of acid-denatured cytochrome c by hydrogen exchange and 2D NMR. *Biochemistry.* 29:10433–10437.

Kataoka, M., Y. Hagihara, K. Mihara, and Y. Goto. 1993. Molten globule of cytochrome c studied by the small angle X-ray scattering. *J. Mol. Biol.* 229:591–596.

Kataoka, M., I. Nishii, T. Fujisawa, T. Ueki, F. Tokunaga, and Y. Goto. 1995. Structural characterization of molten globule and native states of apomyoglobin by solution X-ray scattering. *J. Mol. Biol.* 249:215–228.

Kratky, O., and G. Porod. 1949. Röntgenuntersuchung gelöster Fadenmoleküle. *Rec. Trav. Chim. Pays-Bas.* 68:1106–1123.

Mariani, P., F. Carsughi, F. Spinozzi, S. Romanzetti, G. Meier, R. Casadio, and C. M. Bergamini. 2000. Ligand-induced conformational changes in tissue transglutaminase: Monte Carlo analysis of small-angle scattering data. *Biophys. J.* 78:3240–3251.

Ohgushi, M., and A. Wada. 1983. Molten globule: a compact form of globular proteins with mobile side-chains. *FEBS Lett.* 164:21–24.

Pedersen, J. S., and P. Schurtenberger. 1996. Scattering functions of semi-flexible polymers with and without excluded volume effects. *Macromolecules.* 29:7602–7612.

Pérez, J., P. Vachette, D. Russo, M. Desmadril, and D. Durand. 2001. Heat-induced unfolding of neocarzinostatin, a small all-β protein investigated by small-angle x-ray scattering. *J. Mol. Biol.* 308:721–743.

Pollack, L., M. W. Tate, N. C. Darnton, J. B. Knight, S. M. Gruner, W. A. Eaton, and R. H. Austin. 1999. Compactness of the denatured state of a fast-folding protein measured by submillisecond small angle x-ray scattering. *Proc. Natl. Acad. Sci. U.S.A.* 96:10115–10117.

Rossel, F. I., J. C. Ferrer, and A. G. Mauk. 1998. Proton-linked protein conformational switching: definition of the alkaline conformational transition of yeast iso-1-ferricytochrome c. *J. Am. Chem. Soc.* 120: 11234–11245.

Scott, R. A., and A. G. Mauk. 1996. Cytochrome-c: a multidisciplinary approach. University Science Books, Sausalito, CA.

Semisotnov, G. V., H. Kihara, N. V. Kotova, K. Kimura, Y. Amemiya, K. Wakabayashi, I. N. Serdyuk, A. A. Timchenko, K. Chiba, K. Nikaido, T. Ikura, and K. Kuwajima. 1996. Protein globularization during folding: a study by synchrotron small-angle x-ray scattering. *J. Mol. Biol.* 262: 559–574.

Spinozzi, F., F. Carsughi, and P. Mariani. 1998. Particle shape reconstruction by small-angle scattering: integration of group theory and maximum entropy to multiple expansion method. *J. Chem. Phys.* 109: 10148–10158.

Stuhrmann, H. B., M. H. J. Koch, R. Parfait, J. Haas, K. Ibel, and R. R. Crichton. 1977. Shape of the 50S subunit of *Escherichia coli* ribosomes. *Proc. Natl. Acad. Sci. U.S.A.* 74:2316–2321.

Svergun, D. I. 1997. Restoring three-dimensional structure of biopolymers from solution scattering. *J. Appl. Crystallogr.* 30:792–797.

Svergun, D. I., S. Richard, M. H. J. Koch, Z. Sayers, S. Kuprin, and G. Zaccai. 1998. Protein hydration in solution: experimental observation by X-ray and neutron scattering. *Proc. Natl. Acad. Sci. U.S.A.* 95: 2267–2272.

Svergun, D. I., and H. B. Stuhrmann. 1991. New developments in direct shape determination from small-angle scattering: I. Theory and model calculations. *Acta Crystallogr.* A47:736–744.

Tanford, C. 1970. Protein denaturation (part C): theoretical models for the mechanism of denaturation. *Adv. Protein Chem.* 25:1–9.

Trewhella, J. 1997. Insights into biomolecular function from small-angle scattering. *Curr. Opin. Struct. Biol.* 7:702–708.

Van Holde, K. E., W. C. Johnson, and P. S. Ho. 1998. Principles of physical biochemistry. Prentice Hall, NJ.

Weber, C., B. Michel, and H. R. Bosshard. 1987. Spectroscopic analysis of the cytochrome c oxidase-cytochrome c complex: circular dichroism and magnetic circular dichroism measurements reveal change ot heme geometry imposed by complex formation. *Proc. Natl. Acad. Sci. U.S.A.* 84:6687–6691.

Wilson, M. T., and C. Greenwood. 1996. Cytochrome-c: a multidisciplinary approach. R. A. Scott and A. Grant Mauk, editors. University Science Books, Sausalito, CA. 611–623.